Technical Analyses

1.1 Power Trian Design and Analysis.

In this section, we will conduct a dynamics analysis for the Formula Student car to design the powertrain, and calculate the required mechanical power, motor angular velocity, and torque. The Formula Student car prioritizes safety and roadworthiness, aiming for high acceleration, relatively low maximum speed, and weight. So, the desired performance is to achieve acceleration from 0 to 100 km/h in 5 seconds, a maximum speed of 150 km/h, while maintaining the vehicle mass below the allowed mass of 200 kg.

1.1.1 Mechanical Power Train Topology.

There are three classic arrangements for connecting electric motors and wheels in electric vehicles: central drive with differential, drive closed to the wheel, and wheel hub drive [1]. The mechanical power flow in the central drive with differential topology consists of three main parts: electric motor, reducer, and differential gear. On the other hand, both of Drive closed to the wheel, and wheel hub drive consist of two electric motors and two reducers. The main difference between the last two is in wheel hub drive, the electric motor and the reducer are built inside the wheel where the other one there is a mechanical link to connect the electric motors with the wheels. Shown in Figure 1 [1].

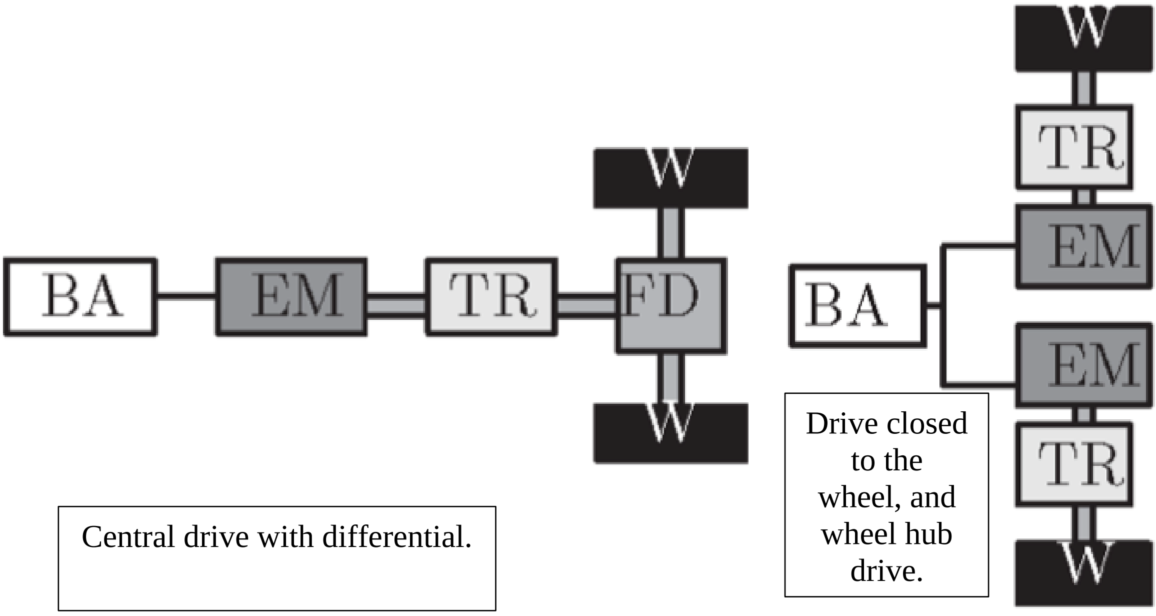

Figure 1 Electric Vehicle Power Train Topologies. [1]

Both Drive close to the wheel and wheel hub drive require two electric motors which results in higher power. Additionally, having a motor for each drive wheel allows for separate control of each wheel. In this way, the torque on each wheel can be controlled individually, creating a more stable vehicle with better steering. However, this arrangement requires two reducers and inverters, which leads to higher costs and weight. Moreover, achieving precise control over the electric motors in these topologies demands a high-performance control unit, very accurate feedback sensors, and advanced programming skills. Table 1 compares the three arrangements based on power, cost, control, and weight.

Table 1 Comparison between the electric vehicles' topologies.

Topology / Comparison	Central drive with differential	Drive closed to the wheel	wheel hub drive
Power	Low	High	High
Cost	Low	High	High
Control	Low	High	High
Weight	Low	High	High

Since this project aims to design a student formula 1 with medium performance and cost. After careful consideration, we have decided that the optimal choice for this car is a central drive with a differential. This option provides a lower cost and weight while still allowing the vehicle to reach the maximum power of 80 kW. In Figure 2, you can see a schematic drawing of the power train we will be using. The electric motor generates the mechanical power, which is then transmitted to the rear wheels through the reducer and the differential gear. Equations 1 and 2 show the relationship between the torque and the angular velocity between the motor and the rear wheels.

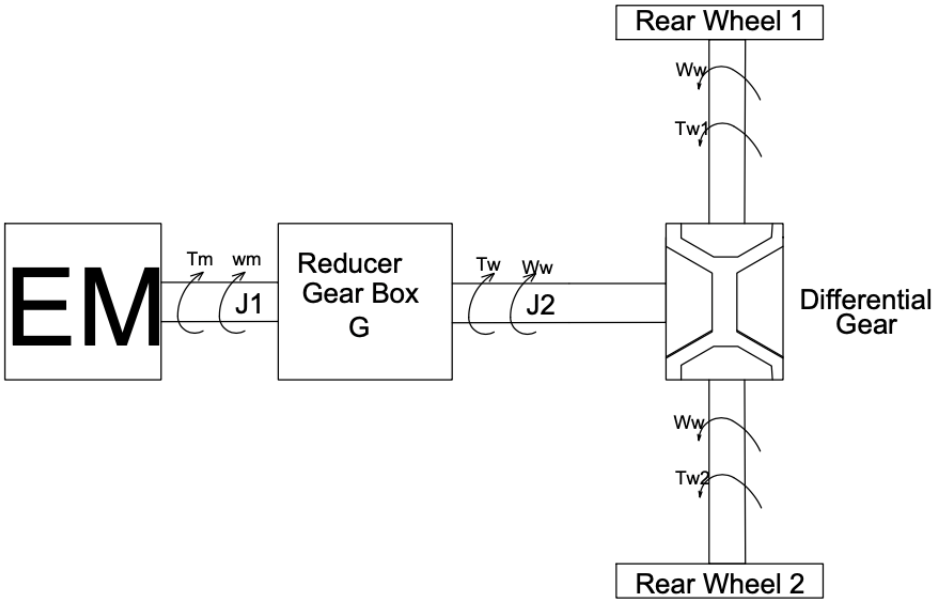

Figure 2 EV Power Train.

$$T_w = T_m \times G \times \eta_G \qquad (1), [2]$$

Where:

- T_w: Total torque on the rear wheels.
- T_m: Torque generated by the electric motor.
- η_G: Total efficiency of the reducer and differential gears.
- G : Reducer gear ratio.

$$\omega_w = \frac{\omega_m}{G} \qquad (2), [2]$$

Where:

ω_w: Angular velocity of the rear wheels.
ω_m: Angular velocity of the electric motor.

1.1.2 Dynamics Analysis.

Figure 3 shows the free-body diagram of the vehicle. The net forces on the car are the driving force generated by the torque on the drive wheels, the air resistance force, and the rolling resistance.

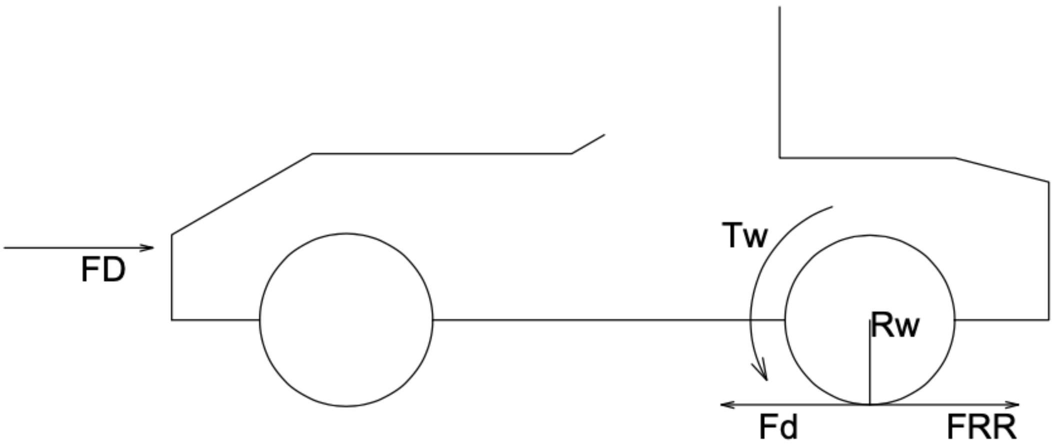

Figure 3 Dynamics Analysis-Free Body Diagram.

By applying the Newton's second law.

$$m\left(\frac{dv}{dt}\right) = F_d - F_D - F_{RR} \qquad (3), [2]$$

Where:

m: vehicle mass with driver.
v: Car linear velocity.
F_{ex}:Total external forces.
F_d: Driving force.
F_D: Drag air resistance.
F_{RR}: Rolling resistance.

$$F_d = \frac{T_w}{R_w} = \frac{T_m \times G \times \eta_G}{R_w} \qquad (4), [2]$$

Where:

R_w: dynamic rolling radius of the tire = 0.2m.

$$F_D = \frac{1}{2}\rho_{air}C_d v^2 A \qquad (5), [3]$$

Where:

ρ_{air}: Air density, 1.265 kg/m^3 at 20 c^o.

C_d: Coefficient of Drag air resistance C_d *assumed at this stage to be* 0.7.

A: Car projected area A *assumed at this stage to be* 1 m^2.

$$F_D = \frac{1}{2}(1.265)(0.7)v^2(1)$$
$$F_D = 0.4427v^2$$

$$F_{RR} = mgcos(\theta)\mu \qquad (6), [3]$$

Where:

g: gravitational acceleration.

μ: rolling resistance coefficient.

θ: Road slope = 0^o.

The rolling resistance coefficient is given as a function of car speed and tyre shown in Figure 4. $\mu = 0.012$ using H tyre type and at 75 mph.

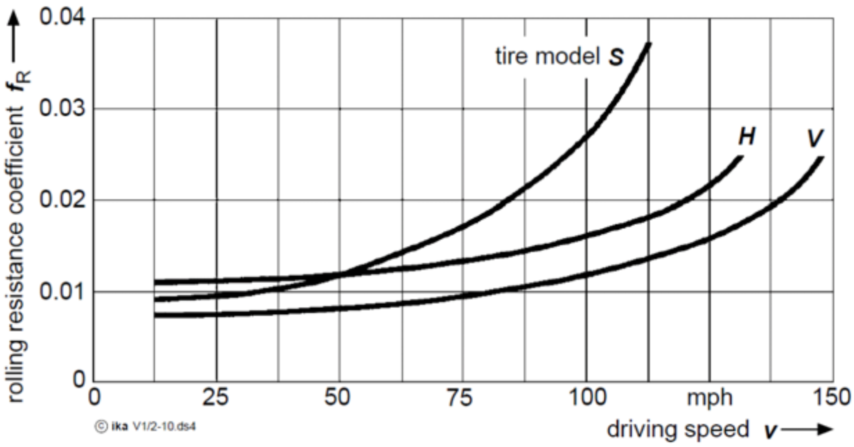

Figure 4 resistance coefficient VS Car speed [4]

$$F_{RR} = (270)(9.81)cos(0)0.012 = 31.8\ N$$

For a 70 kg driver, $m = 270\ kg$:

Equation (3):

$$m\left(\frac{dv}{dt}\right) = F_d - F_D - F_{RR}$$

$$270\left(\frac{dv}{dt}\right)=\frac{T_w}{0.2}-0.4427v^2-31.8$$

$$\frac{dv}{\frac{T_w}{0.2}-0.4427v^2-31.8}=\frac{dt}{270} \tag{7}$$

Taking the integral to calculate the required torque on the wheels to generate acceleration from 0 to 100 km/h in 5 s.

$$\int_0^{27.78}\frac{dv}{\frac{T_w}{0.2}-0.4427v^2-31.8}=\int_0^5\frac{dt}{270}$$

$$T_w=330\ N.m$$

$$\omega_w=\frac{\omega_m}{G}$$

The average efficient maximum speed for electric motors used in the automotive is between 6000 to 20000 RPM. However, the higher the speed, the higher the cost is required. So, we are going with a low-speed motor with a max speed of 7000 RPM.

The desired car velocity is 150 km/h:

$$150\,\frac{\text{km}}{\text{h}}=150\,\frac{1000}{3600}\frac{m}{s}=41.67\ \text{m/s}$$

$$v=\frac{\omega_m(RPM)\times\left(\frac{2\pi}{60}\right)}{G}\times R_w$$

$$41.67=\frac{7000\times\left(\frac{2\pi}{60}\right)}{G}\times 0.2=\frac{146.53}{G}$$

$$G=3.5$$

$$T_w=T_m\times G\times\eta_G$$

The average velocity of the Spur and Helical gears is between 98% to 99% if the reduction ratio is less than 6.6. So, we will take $\eta_G=0.98$ [5].

$$330=T_m\times 3.5\times 0.98$$

$$T_m=96\ \text{N.m}$$

To find the required torque to overcome the aerodynamics and rolling resistance at the car max speed (150 km/h or 41.67 m/s):

$$F_d = F_D + F_{RR}$$

$$\frac{T_m \times 3.5 \times 0.98}{0.2} = 0.4427v^2 - 31.8,\ sub\ v = \ 41.67 \text{ m/s}$$

$$T_m = 43\ N.m$$

1.1.3 Motor Selection.

Table 2 outlines the main performance requirements to achieve the required car's acceleration and speed.

Table 2 The required motor's performance.

Peak Torque (N.m)	96
Continues Torque (N.m)	43
Maximum continues angular velocity (RPM)	7000

There are four different motors used in electric car applications, which are: DC motors, Induction Motors (IM), Permanent Magnet Synchronous motors (PMSM), and Switch Reluctance motors (SRM). To choose the optimal motor for our application, a comparison between these types based on cost, weight, size, controllability, efficiency, and maximum torque. To make the comparison easier, we will use a scale of 1 to 4, with 4 being the best, to determine the ideal choice.

Table 3 Comparation between types of motors used in EVs [6] [7].

	DC motor	(IM)	PMSM	SRM
Cost	2	3	1	2
Power Density	1	2	3	3
Size	2	2	3	1
Controllability	4	4	3	2
Efficiency	1	2	3	3
Maximum Torque	2	2	3	3
SUM	12	15	16	14

Based on Table 3, the most optimal option based on our requirements is Permanent Magnet Synchronous Motor (PMSM). A PMSM with the closest performance to our requirements is EMRAX 188, which offers 100 N.m peak torque for 10 seconds, 50 N.m as continuous torque, and a rated angular velocity of 7000 RPM [8]. It provides three input voltage options (Low 100 DC, Medium 270 DC, and High Voltage 400 DC). The manufacturing company offers the Low Voltage motor for 2910 £ and 2410 € for the second two options. So, the choice with lower cost is having the one with low input voltage since having a high voltage will increase the cost of the battery significantly.

1.1.3.1 Acceleration Test

A simulation will be conducted in this section to evaluate the dynamic response achieved using the chosen electric motor. Figures 5 and 6 were obtained through the dynamic vehicle simulation presented in Figure 10. Figure 5 illustrates the relationship between the vehicle speed and motor angular velocity over time when applying the maximum continuous torque of 50 N.m for 40 seconds. The time required to accelerate from 0 to 100 km/h is 11 seconds.

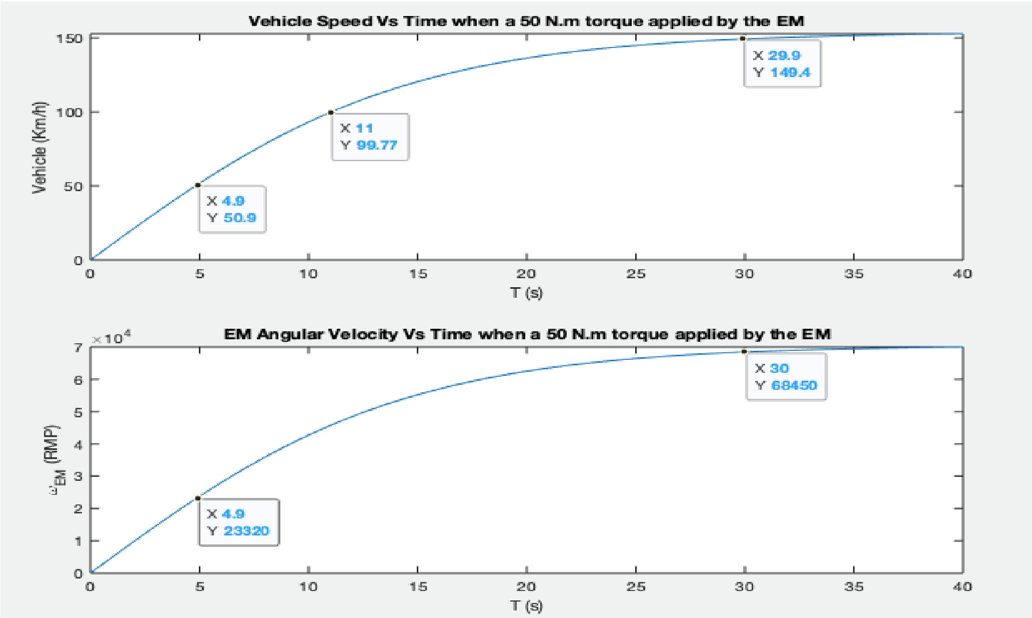

Figure 5 Vehicle Speed and EM AV Vs Time when a 50 N.m torque applied by the EM for 40 s.

To improve acceleration, a peak torque of 100 N.m will be applied for 5 seconds. After that, the power will be switched back to continuous to avoid any damage to the electromagnetic motor. The outcome of this input torque is displayed in Figure 6, which shows that the car can reach a speed of 100 km/h in just 5 seconds. The maximum speed achievable is 152 km/h when the EM angular velocity is 7000 RPM, which happens to be the maximum continuous angular velocity for the selected motor.

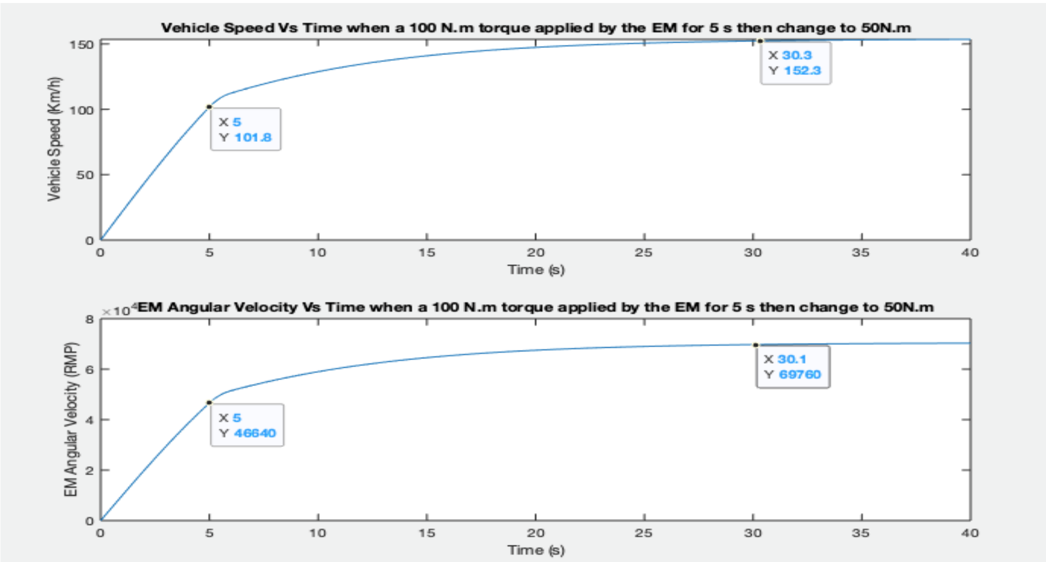

Figure 6 Vehicle Speed and EM AV Vs Time when a 100 N.m torque applied by the EM for 5 s then dropped to 50N.m for 35 s.

1.1.4 Battery Selection.

Battery selection significantly impacts the cost, safety, sustainability, and weight of Formula Student. Lithium Ionic cell A123 AMP20M1HD is the most suitable choice for FS application. Although it costs more than other types of batteries, it has slower self-discharging, longer life span, less CO2 emission during its life cycle, and higher energy density. Table 5 compares various battery types based on the mentioned variables.

Table 4 Comparison of lithium-ion batteries with other types [10] [11].

Specifications	Lead Acid	Ni-Cd	Ni-MH	Lithium Ionic
Self-Discharge [10]	High	Moderate	Low	Very Low
Cycle Life [10]	200-300	1500	300-500	500-1000
Life-cycle Environmental Impact [11]	100	108	97.7	55.2
Energy Density (w/kg) [10]	30-50	45-80	60-120	110-160

To design a battery pack for the EMRAX 188 EM motor, we use Li A123 AMP20M1HD-A cells. The pack needs to provide 100 volts, 400 amps of continuous current, and 800 amps of peak current to satisfy the EM requirements. To achieve the desired voltage, we will connect the cells in series within a package. Then, we will connect these packages in parallel to achieve the required current.

Each cell of Li A123 AMP20M1HD-A provides 3.3 V and 350 A [12].

$$V_{req} = V_{cell} \times N_s$$

Where:

V_{req}: The required output Voltages (100 V).
V_{cell}: The cell's output Voltage (3.3V).
N_s: number of cells required to be connected in series.

$$N_s = \frac{V_{req}}{V_{cell}} \approx 30$$

$$I_{req} = I_{cell} \times N_p$$

Where:

I_{req}: The required output Current (800 A).
I_{cell}: The cell's output Current (350 A).
N_p: Number of packages required to be connected in parallel.

$$N_p = \frac{I_{req}}{I_{cell}} \approx 3$$

It is also essential to assess the energy demands for the planned application. This involves determining the necessary battery capacity, considering the specified 22 km travel distance, and accounting for energy losses during braking and acceleration by taking throttle and brake angles shown in Figure 7 as input, which simulate the performance of the proposed vehicle on the Silverstone racing circuit in order to complete 4 rounds [14]. The required capacity can be found through the integration of current over time from the start to the target distance, which shown in description of computer code section. To account for potential variations in driver behaviour, a conservative approach is adopted, designating a 25 km travel distance with a 3 km Factor of Safety.

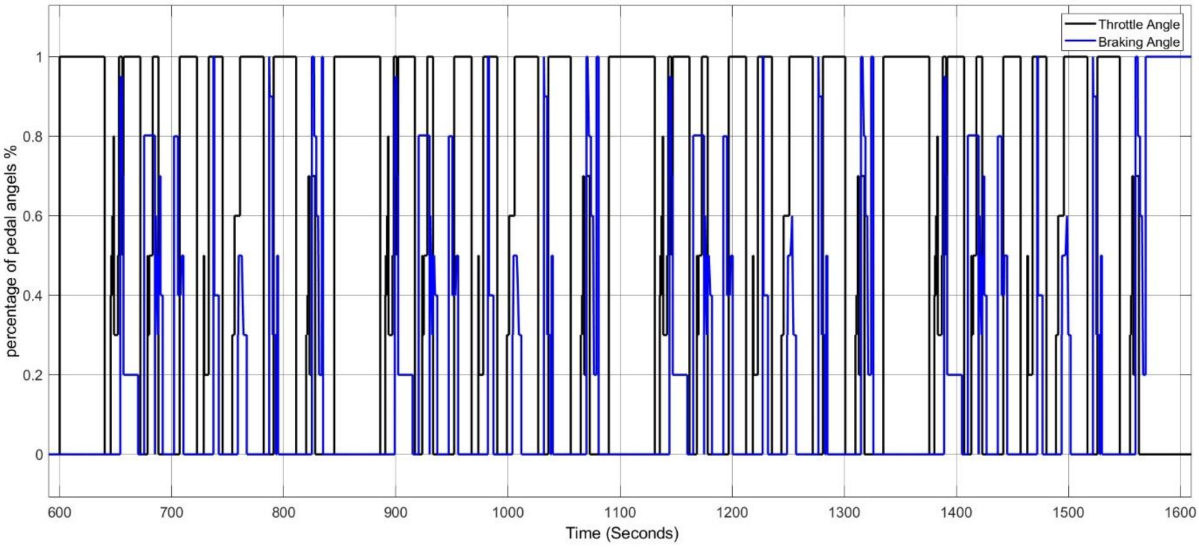

Figure 7Braking and Throttle angles.

After applying these inputs, the distance travelled by the vehicle is found to be 25 km and the vehicle consumed 70 Ah. So, the battery capacity should be more than 70 Ah.

$$C_B = C_{cell} \times N_c$$

Where:

C_{req}: The battery capacity (Ah).
C_{cell}: The cell's capacity (19.6 Ah).
N_c: Number of packages required to be connected in parallel.

$$N_c = \frac{C_{req}}{C_{cell}} = 3.56$$
$$N_c = 4$$

So, the number of packages required to be connected in parallel to provide the required current and capacity is four. Also, the number of cells required to be connected in series to provide the required voltage is 30 cells.

Description of Computer Code

We used MATLAB Simulink to simulate the behaviour of our vehicle. Figure 6 shows the Simulink diagram of the entire system, which includes a Battery Management System (BMS), a model of the high-voltage battery, and the vehicle's dynamic behaviour. The BMS controls the current that charges or discharges the battery, while the battery model simulates the voltage, state of charge (SOC), and temperature status of each cell of the battery. The vehicle dynamics part takes the current from the battery as input and calculates the vehicle's acceleration, velocity, and distance travelled over time.

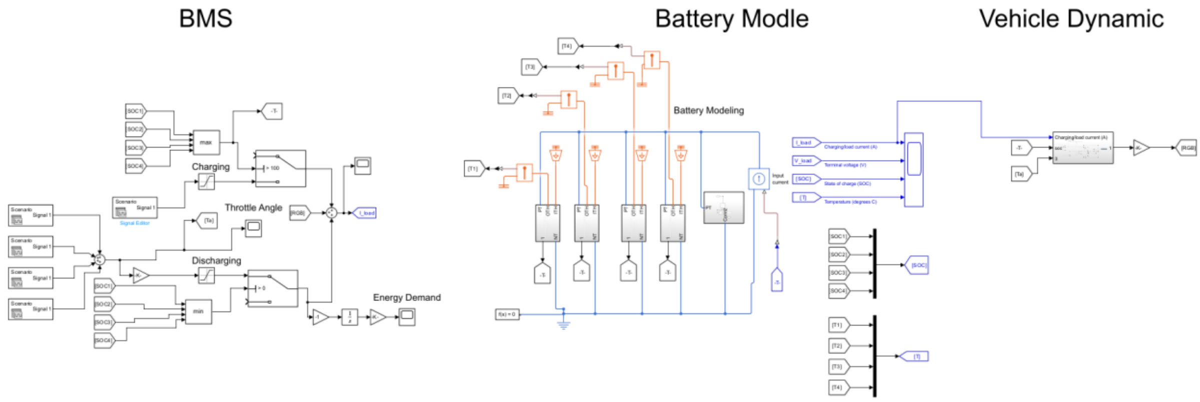

Figure 8 MATLAB Simulink simulation.

1 Battery Management System

Figure 7 shows the Simulink model of the Battery Management System (BMS) used in our vehicle. This system determines the charging and discharging procedures considering several parameters such as the state of charge (SOC), cell temperature, and inputs from the throttle and brake pedals.

Signal Editor 5 has now introduced a new charging protocol which involves a 320 A current taken from a 100 V DC source to charge the high-voltage battery. However, two critical conditions must be met before initiating the charging process. Firstly, the temperature of the battery cells should remain below 65°C and secondly, the SOC (State of Charge) should not exceed 100%.

The output of signal editors 1-4 corresponds to the throttle angle, as shown in Figure 5. This output modulates the inverter, which regulates the discharging current, and provides the required current to the electric motor. Our operational policy ensures that the motor receives an initial surge of 800A for the first 5 seconds when the throttle is fully engaged. Afterwards, the current drops to a sustained 400A for full throttle and a proportional adjustment for partial engagement. Similarly, the discharging mechanism is also temperature-dependent and requires a positive SOC across all cells.

The combined input of these currents, alongside the regenerative braking current, is channelled to the battery model through the 'I-load' label. In this part, the required battery capacity was calculated by integrating the current associated with the given throttle position, the results of which are visualized in the "Energy Demand" scope.

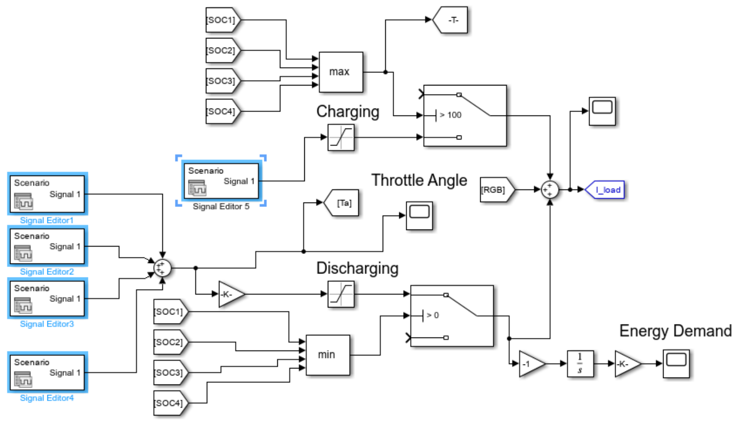

Figure 9 Charging & Discharging policy.

2 Battery Model.

Figures 8 and 9 display a detailed electrical schematic of our battery modelling system built with MATLAB Simulink. This model is designed to imitate a battery array, which consists of four packages (Figure 9), each holding 30 lithium-ion A123 AMP20M1HD-A battery cells (Figure 8) connected in series. The battery charges, discharges, and regenerative braking produce the current, which is then used to charge and discharge the overall battery, while the battery's overall voltage is monitored by the voltage sensor. Each cell in the package generates heat during its operation, which is then conducted from one cell to another facilitated by direct contact over an area of 0.0393 square meters. The final cell in the series dissipates this cumulative heat primarily via free convection into the environment maintained at 20 degrees Celsius. The model includes thermocouples (T1, T2, T3, and T4) for temperature monitoring and control blocks to simulate the electrical behaviour and heat generation within each cell.

For each branch, the system calculates the state of charge (SOC) in response to an input current signal. The schematics determine the average SOC for all cells within a package and display it on the primary scope.

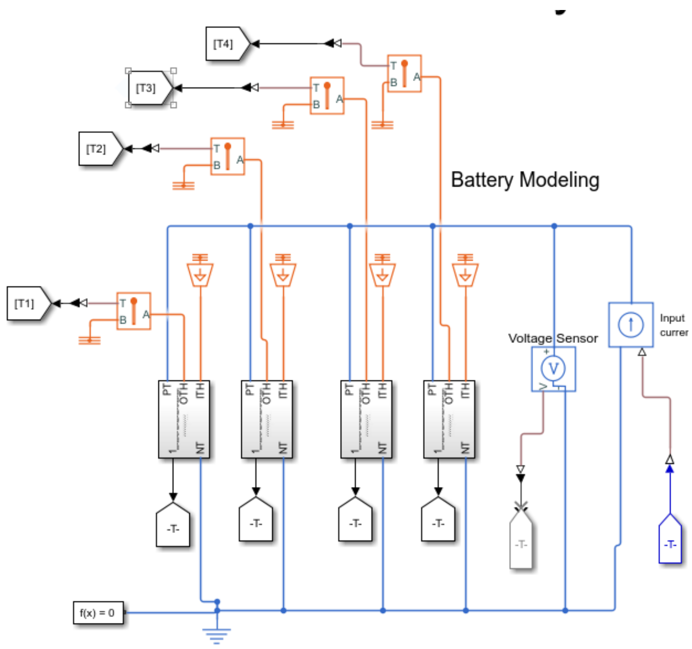

Figure 11 Model of the High-Voltage Battery

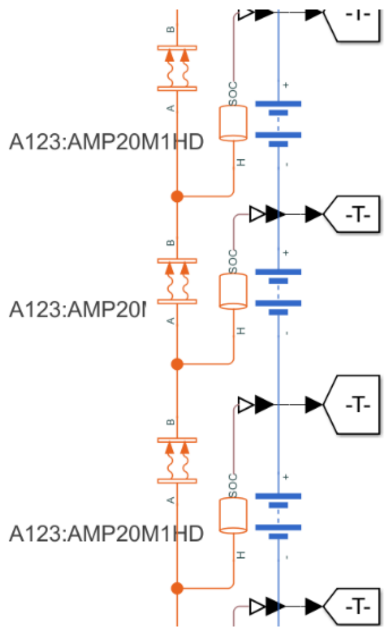

Figure 10 One package consists of 30 series cells.

3 Vehicle Dynamics Simulation

This simulation is crucial for understanding how the output of the electrical system (battery current) affects the mechanical response of the vehicle (motion dynamics). Figure 10 shows the system that considers the current and braking angle to calculate the acceleration, speed, and position of the vehicle over time. The transfer function in Figure 11 is used to calculate these values, where the sum sign sums the driving force, the aerodynamics, and the rolling resistance forces. The forces are given in equation (9). The velocity in the aerodynamics resistance part is obtained by integrating acceleration, and the motor torque is found from the current using equation (10), which is provided on the electric motor datasheet [8]. The braking force is obtained from the regenerative and mechanical braking torques, which depend on the type of brake and vehicle speed. However, in this simulation, we assume it to be the percentage of the braking angle multiplied by 50 N.m for simplicity.

$$\sum F = 17.15T_m - 0.4427v^2 - 31.8 - braking\ force \tag{9}$$

$$T_m = \frac{0.15}{\sqrt{2}} \times I \tag{10}$$

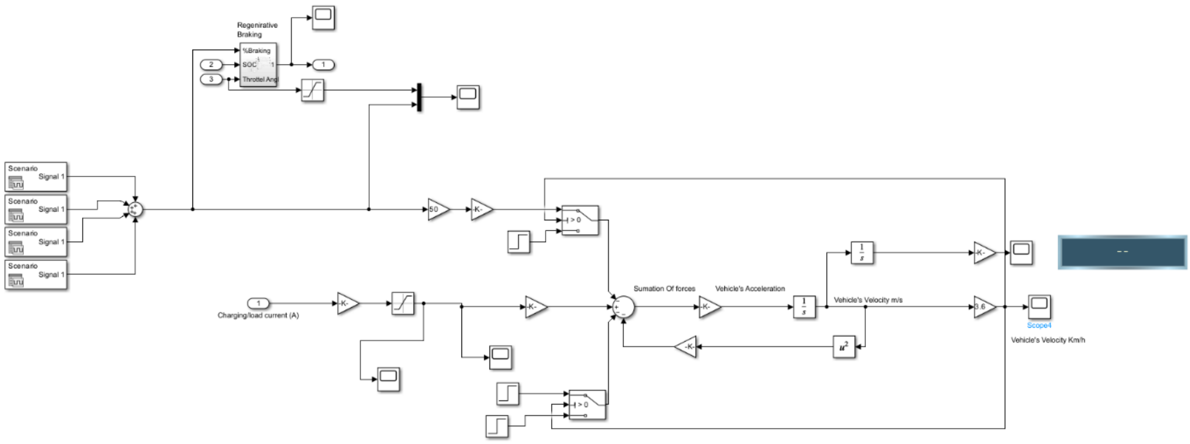

Figure 12 Simulink simulation of the vehicle dynamics behavior.

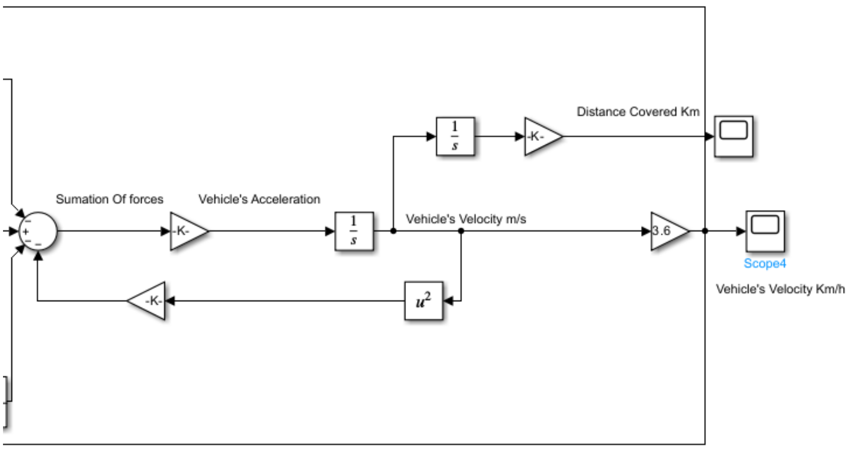

Figure 13

4 Regenerative braking

Regenerative braking is a method of recovering energy that converts a vehicle's kinetic energy into electrical energy, which can then be stored in the vehicle's battery system. In our system, Figure 12 shows how regenerative braking works. When certain conditions are met, it causes the rotating magnetic flux (RMF) speed to be less than the rotor speed, which generates electricity from the vehicle's kinetic energy. The conditions in our model include the battery's state-of-charge (SOC) being less than 80%, the braking angle being greater than zero, the battery temperature being within the allowed range, and the throttle angle being zero.

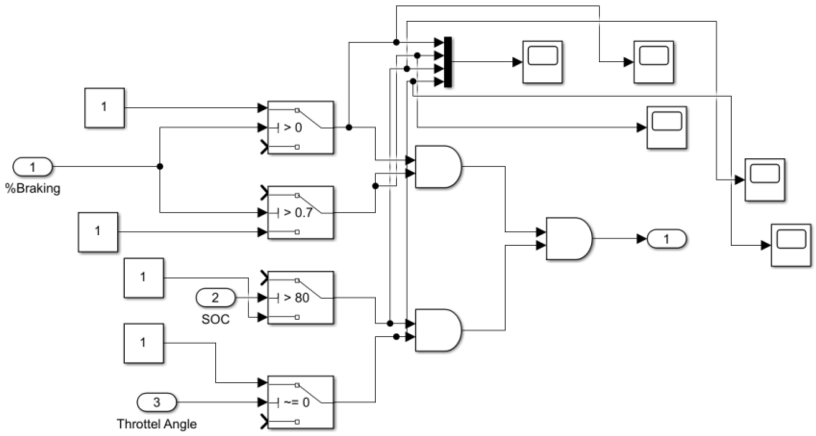

Figure 14 Regenerative braking Simulink.

5 Simulation Results

The Simulink simulation was conducted to evaluate the performance of the Formula Student vehicle which has yielded significant results. The vehicle was able to complete the designated 23 km path of the FS dynamics event within 16 minutes, showcasing its ability to maintain high speeds and efficiency throughout the event (as shown in Figure 13).

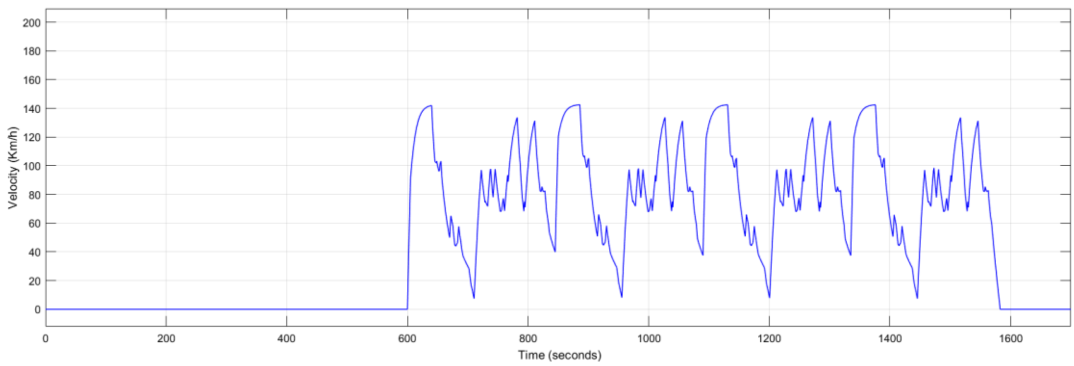

Figure 15 Vehicle Speed

Furthermore, the vehicle's battery state of charge (SOC) was observed to be 25% after the dynamics event (as shown in Figure 14). This SOC level is critical in understanding the energy consumption patterns of the vehicle under race conditions and suggests a balanced energy usage strategy that could potentially be optimized for future events to either increase performance or endurance.

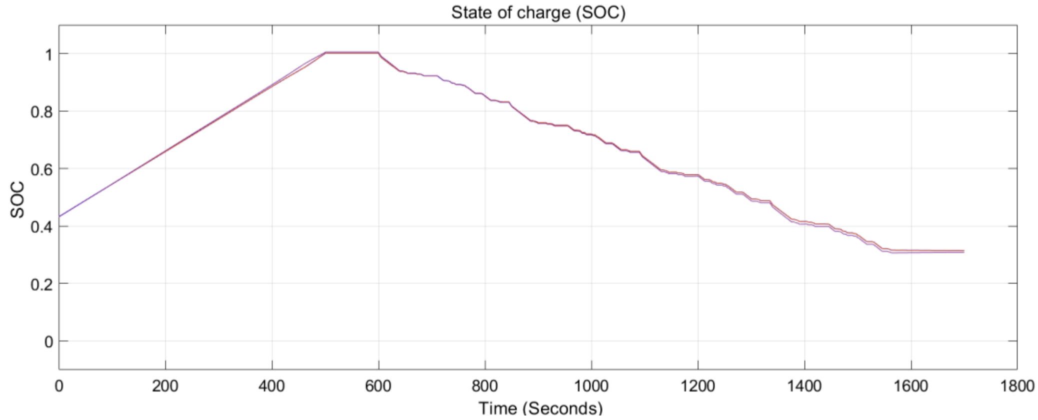

Figure 16 State of Charge.

The temperature management system of the vehicle also demonstrated effective performance. The recorded temperature was 20°C below the critical threshold of 65°C (as shown in Figure 15) after completing the dynamics simulation. This margin indicates a robust thermal management system that successfully kept the vehicle's operating temperatures within safe limits, thereby ensuring both the integrity of the vehicle's components and the safety of the operation.

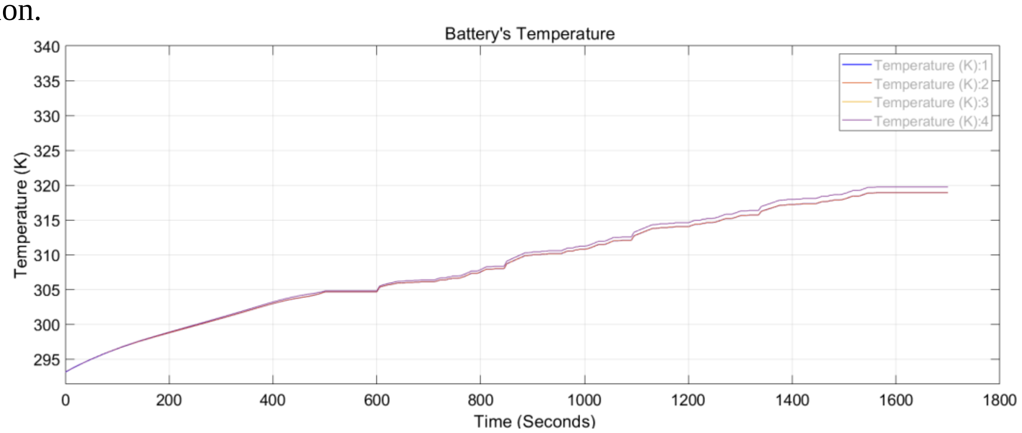

Figure 17 Battery's Temperature.

In this simulation, Figure 16 represents the charging and discharging current of the battery. The battery initially charged from 40% to 100% SOC using the positive 320 A charging signal. Once the motor turns on, it starts consuming current based on the throttle angle. Furthermore, the regenerative braking system played a vital role in confirming the vehicle's energy efficiency through the generation of regenerative current during braking phases.

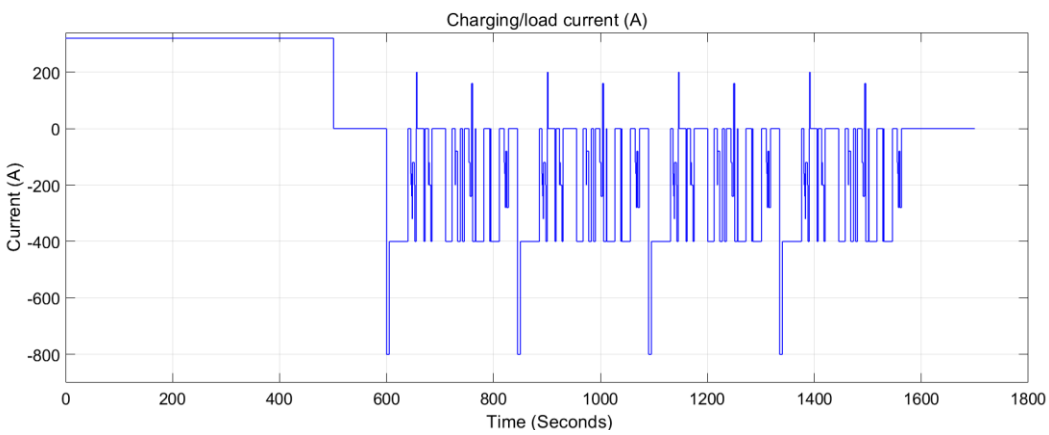

Figure 18 High-Voltage Current.

Lastly, Figure 17 provides a detailed view of the terminal voltages of our battery during the dynamics event. Tracking the terminal voltages is crucial for assessing the health status of the battery. It helps in understanding the uniformity of cell voltages, potential cell degradation, and overall battery efficiency under load conditions. The information depicted in Figure 17 is essential to ensure that the battery operates within its optimal voltage range, safeguarding its longevity and performance. This analysis is vital for ongoing maintenance and development efforts, as it helps in identifying any discrepancies early on that could affect the vehicle's performance or safety during the competition.

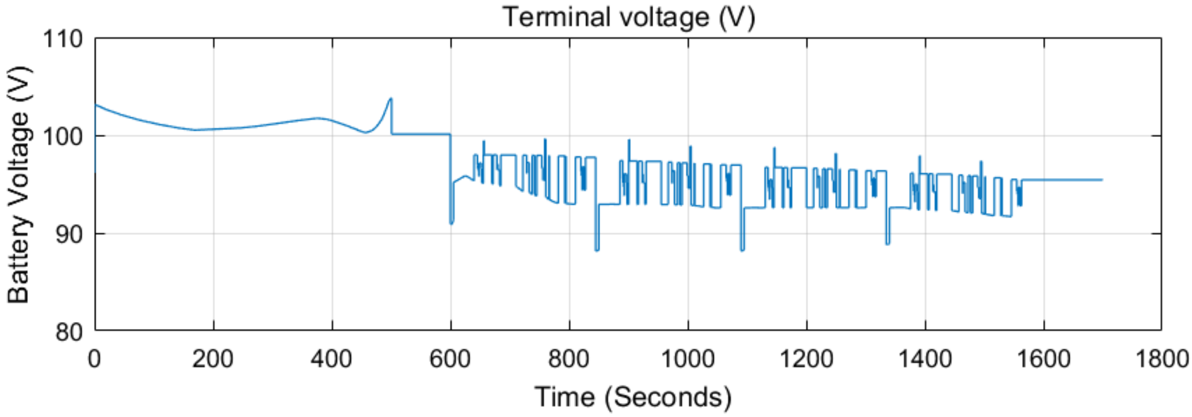

Figure 19 High-Voltage Battery Terminal Voltage.

Bill of Materials

The selected EMRAX 188 Package is shown in Table 4.

Table 5 The specification and cost of the selected EMRAX [9].

System	Cost £	Quantity	Total Cost
EMRAX 188 Single motor	2410	1	2410
Low Voltage (100V)	500	1	500
Air Cooled	0	1	0
For radial-axial forces; pull-push mode	0	1	0
Standard motor shaft	0	1	0
Encoder RM44SC on back of the motor	390	1	390

System	Cost £	Quantity	Total Cost
A123 AMP20M1HD	20	120	2400
Coroflex flexible orange battery cable	45/m	-	-
Reducer Gearbox 3.5:1	200	1	200
Back Axle	140	1	140

Technical Diagrams:

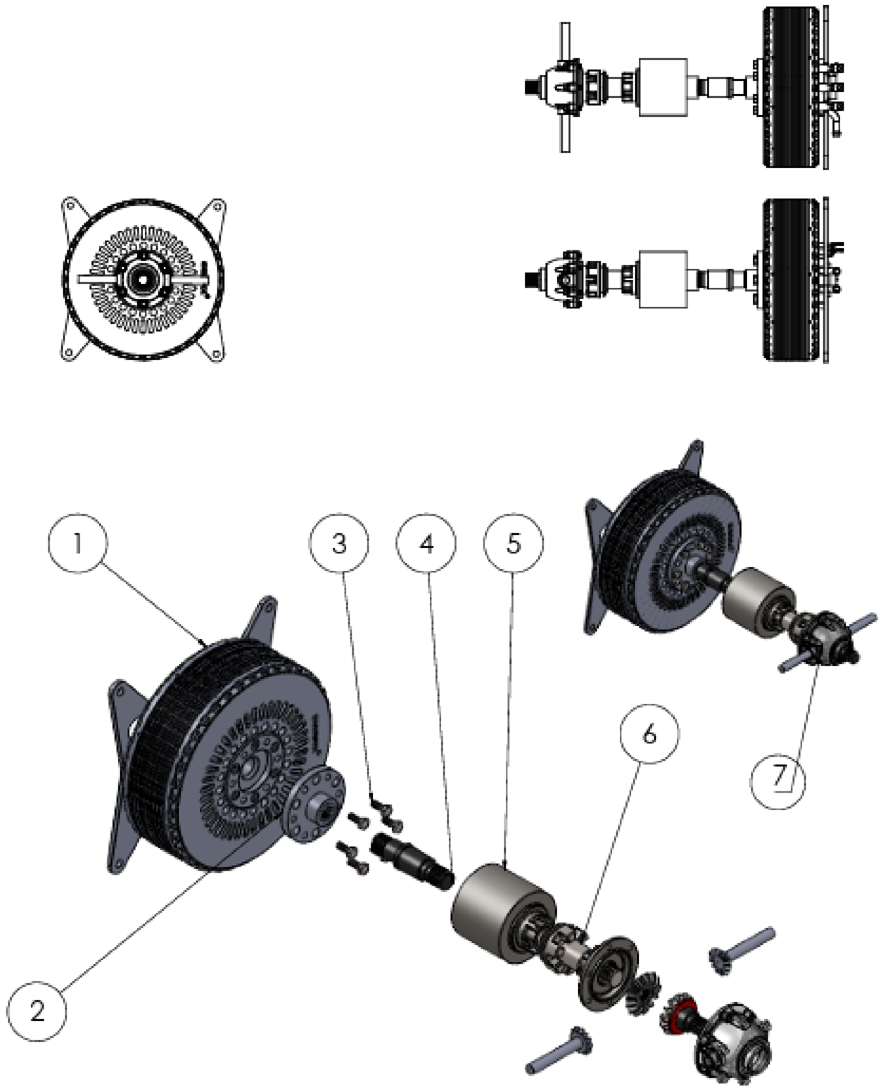

ITEM NO.	DESCRIPTION	QTY.
1	EMRAX188 Electric Motor	1
2	Motor-Drive shaft link	1
3	B18.2.3.2M - Formed hex screw, M8 x 1.25 x 20 --20WS	1
4	Drive Shaft	1
5	Reducer Gearbox 3.5:1 Rasio	1
6	Reducer-Back Axle Link	1
7	Back Axle	1

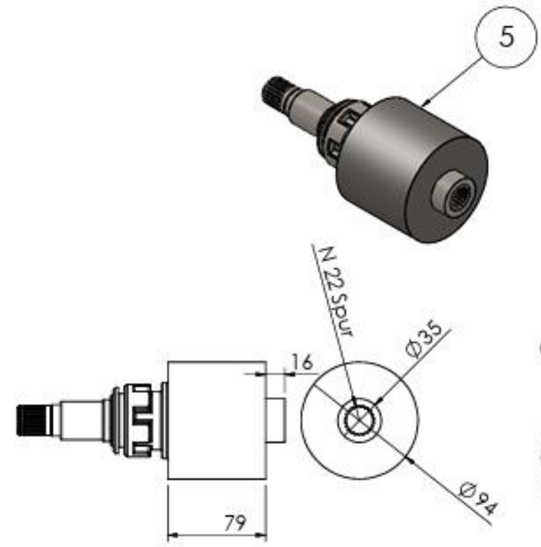
5
N 22 Spur
Ø35
16
Ø94
79

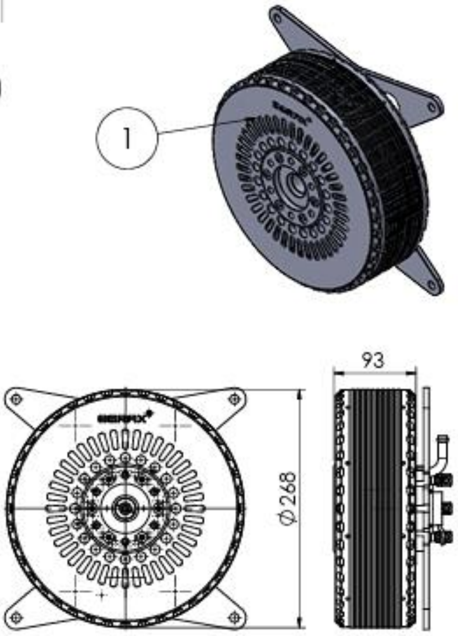
1
93
Ø268

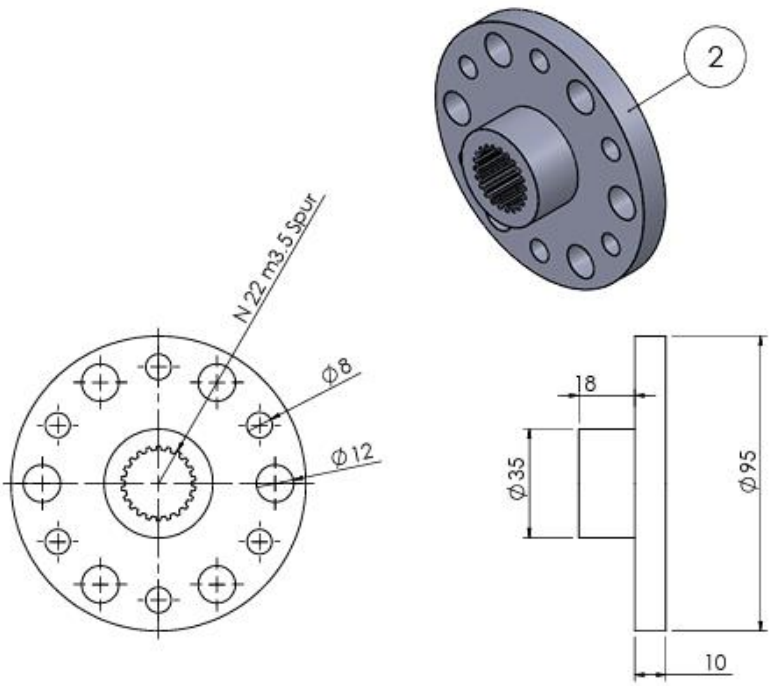
2
N 22 m3.5 Spur
Ø8
Ø12
18
Ø35
Ø95
10

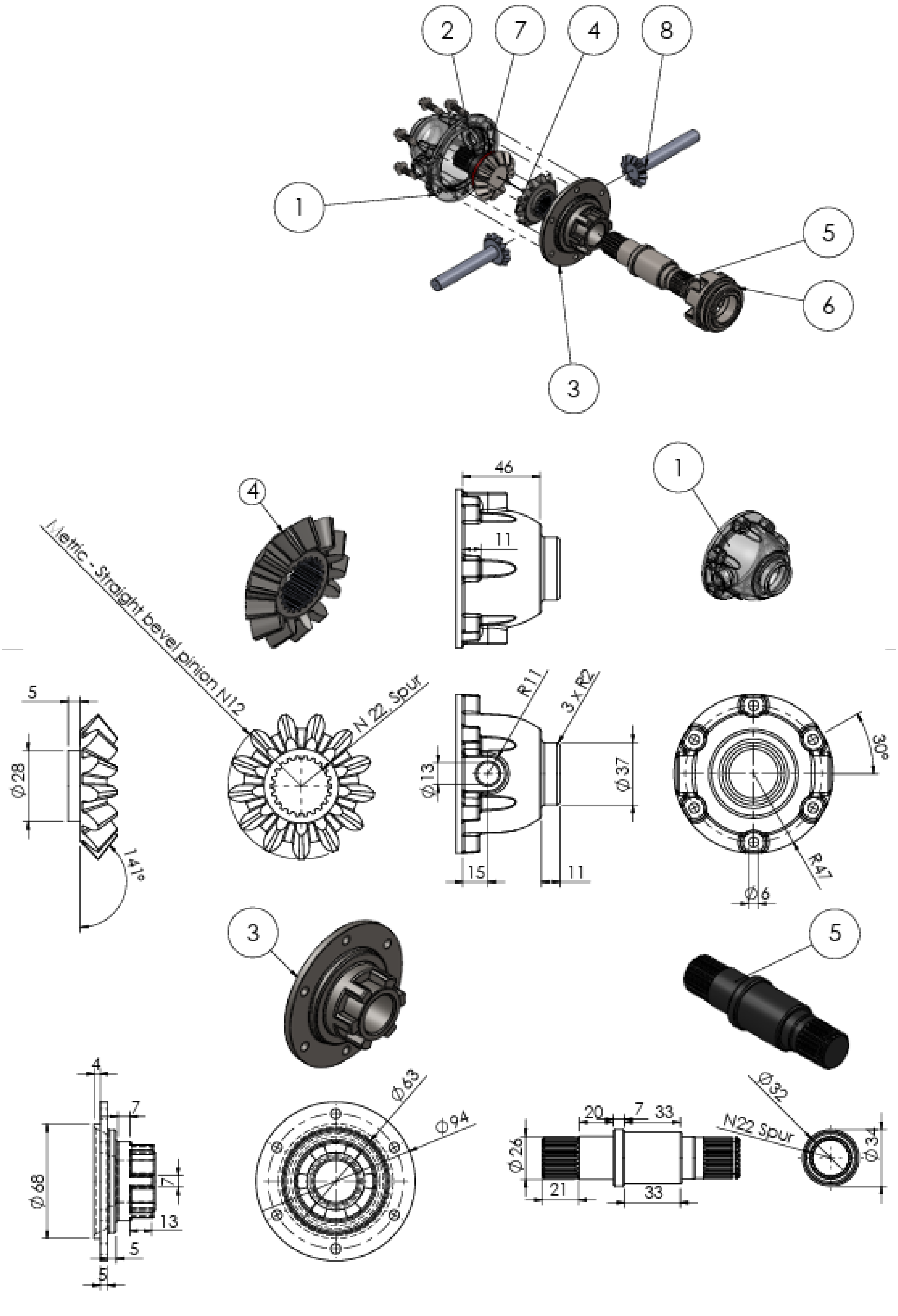
2
7
4
8
1
5
6
3
46
11
Metric - Straight bevel pinion N12
N 22, Spur
R11
3 x R2
Ø13
Ø37
15
11
30°
R47
Ø6
5
Ø28
141°
4
7
7
Ø68
13
5
5
Ø63
Ø94
20
7
33
Ø26
21
33
Ø32
N22 Spur
Ø34

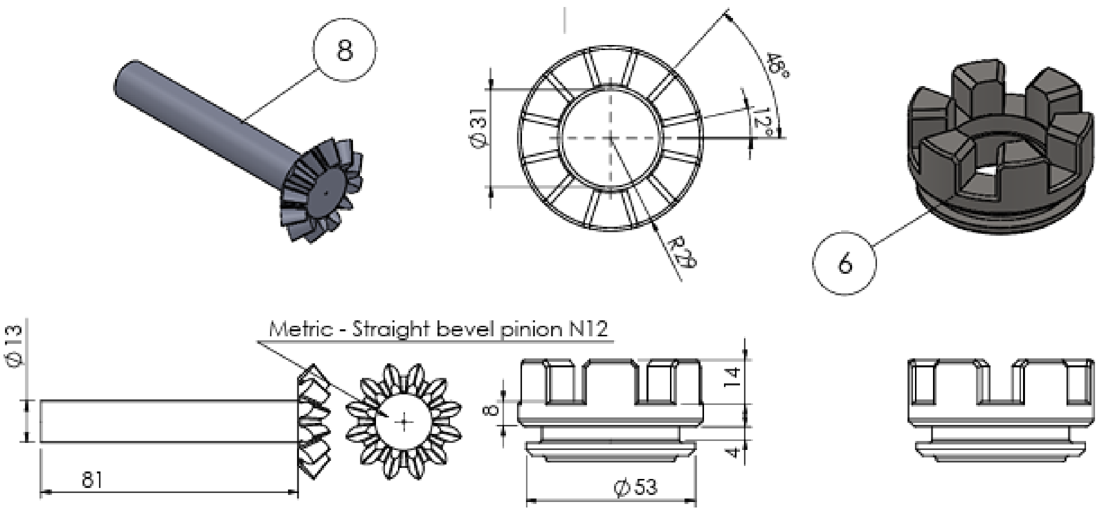

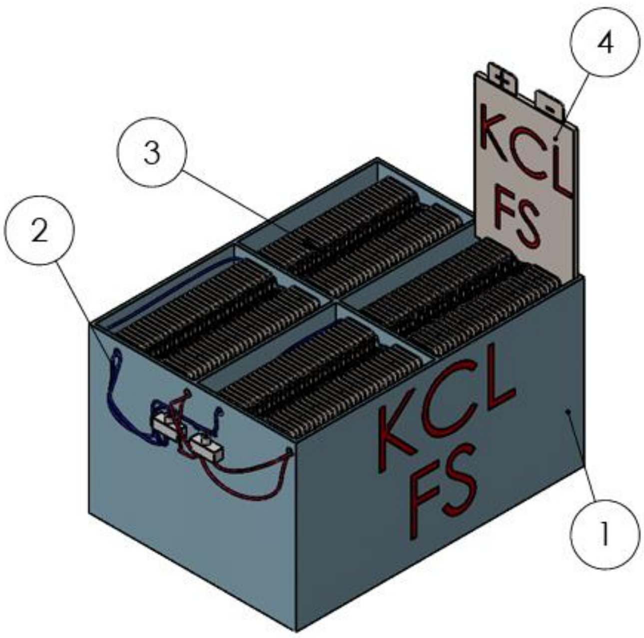

ITEM NO.	DESCRIPTION	QTY.
1	Battery Case	1
2	Coroflex flexible Orange battery cable	-
3	Battery Package	4
4	Li A123 AMP20M1HD-A Cell	120

References

[1] E. S. a. T. H. Frans J. R. Verbruggen, “MDPI,” Electric Powertrain Topology Analysis and Design for Heavy-Duty Trucks, 31 10 2023. [Online]. Available: https://www.mdpi.com/1996-1073/13/10/2434.

[2] R. C. Hibbeler, Engineering Mechanics, Dynamics, FOURTEENTH EDITION.

[3] J. S. a. J. Cha, “Analysis of Driving Dynamics Considering Driving Resistances in On-Road Driving,” *MDPI,* 2021.

[4] “How to calculate rolling resistance,” X-Engineering, [Online]. Available: https://x-engineer.org/rolling-resistance/. [Accessed 17 10 2023].

[5] Roymech.org, “Gear Efficiency,” 2020. [Online]. Available: https://roymech.org/Useful_Tables/Drive/Gear_Efficiency.html. [Accessed 22 11 2023].

[6] A. S. J. Khalid S. Mohammad, “Comarison between electic motors used in electric vehicle propulsion system,” *Indonnesian Journal of Electrical Engineering and Compuer Science,* vol. 20, 2022.

[7] M. Verma, “Study about the DC Machine and Analyse Torque-Speed Characteristics of DC Motor and Comparison of different types of Electric Motors used in EV.,” [Online]. Available: https://skill-lync.com/student-projects/bldc-motor. [Accessed 22 11 2023].

[8] EMRAX, “EMRAX 188 Technichal data table,” 8 2018. [Online]. Available: https://emrax.com/wp-content/uploads/2016/12/emrax_188_technical_data.pdf. [Accessed 22 11 2023].

[9] J.-M. T. J. V. M. S. M. J a Matheys, “Comparison of the Environmental impact of 5 Electric Vehicle Battery technologies using LCA,” Jan 2009. [Online]. Available: https://www.researchgate.net/publication/234162894_Comparison_of_the_Environmental_impact_of_5_Electric_Vehicle_Battery_technologies_using_LCA. [Accessed 17 Jan 2024].

[10] H. M. I. I. Muhammad Nizam, “Constant current-fuzzy logic algorithm for lithium-ion battery charging,” June 2022. [Online]. Available: https://www.researchgate.net/publication/360937364_Constant_current-fuzzy_logic_algorithm_for_lithium-ion_battery_charging. [Accessed 17 Jan 2024].

[11] 2. A. Systems, “ Lithium Ion Prismatic Pouch Cell AMP20M1HD-A,” 2021. [Online]. Available: https://www.buya123products.com/uploads/vipcase/468623916e3ecc5b8a5f3d20825eb98d.pdf. [Accessed 29 11 2023].

[12] A. Covelli, “Githup,” fastest-lap, 8 2023. [Online]. Available: https://github.com/juanmanzanero/fastest-lap. [Accessed 7 2 2024].

[13] EMRAX, “Inquiry through email (support@emrax.com),” 2023.

[14] V. Jacob, “nternational Journal of Innovative Science and Research Technology,” 6 2021. [Online]. Available: https://ijisrt.com/assets/upload/files/IJISRT21JUN852.pdf. [Accessed 31 10 2023].